Accurate Curvature Estimation along Digital Contours with Maximal Digital Circular Arcs

Tristan Roussillon[1] and Jacques-Olivier Lachaud[2]

[1] Université de Lyon,
Université Lyon 2, LIRIS, UMR5205, 69676, France
tristan.roussillon@liris.cnrs.fr
[2] LAMA, UMR CNRS 5127
Université de Savoie, Le Bourget-du-Lac, 73376, France
jacques-olivier.lachaud@univ-savoie.fr

Abstract. We propose in this paper a new curvature estimator based on the set of maximal digital circular arcs. For strictly convex shapes with continuous curvature fields digitized on a grid of step h, we show that this estimator is mutligrid convergent if the discrete length of the maximal digital circular arcs grows in $\Omega(h^{-\frac{1}{2}})$. We indeed observed this order of magnitude. Moreover, experiments showed that our estimator is at least as fast to compute as existing estimators and more accurate even at low resolution.

1 Introduction

The accurate estimation of geometric parameters such as perimeter, tangent and curvature along digital objects is important for many image analysis applications, for instance the detection of dominant points and corners. We focus here on curvature estimation along digital contours, assumed to be digitizations of smooth Euclidean shapes of the plane. This subject has led to the development of many estimators, which fall roughly in three categories according to [17,16,8]: (i) derivative of the tangent orientation, (ii) norm of the second derivative of the curve considered as a path, (iii) inverse of the osculating circle radius. In most approaches, a user-given window or smoothing parameter is used so as to remove the jaggedness of digital contours and to make it continuous [17,16,4,12,13,3,5,6].

In approaches of (i), the curvature estimation relies on the convolution of the contour tangent by some derivative of Gaussian kernel, either in a continuous setting [17,16,4], or in a discrete setting [13,3,5]. Furthermore a preprocessing with digital straight segments is sometimes used to limit the arithmetic effects [16,4]. Methods of (ii) generally reconstruct locally the contour with some polynomial of given degree [14,8]. Again, an important parameter is the size of the window. Methods of (iii) tries to estimate the osculating circle around the point of interest [1,2,8,6].

Among all these curvature estimators, few do not require an external parameter. They all rely on digital straight segment (DSS) recognition. Only the length of DSS is used in [1] to estimate the osculating circle, but this approach

J.K. Aggarwal et al. (Eds.): IWCIA 2011, LNCS 6636, pp. 43–55, 2011.

does not give accurate estimations. In [2] (HK2005 in [8]), the two half-tangents define a triangle whose circumscribed circle approximates the osculating circle. This technique gives correct results on average, but oscillates a lot and leads to very large errors as reported in [9]. The GMC estimator [9] computes, among all Euclidean shapes that are digitized as the input digital shape, the shape that minimizes its squared curvature. Digital straight segments are used here as a preprocessing to make easier the optimization.

An important property that should have a discrete estimator is the *multigrid convergence* [10]. Indeed, at a given resolution, infinitely many shapes have the same digitization, which hampers the objective comparison of estimators. For estimators of local geometric quantities like tangent or curvature, few results exist. We may quote some convergence results for tangent estimators [11,13,3]. And there is no correct convergence results for curvature as far as we know.

In this paper, we present in Section 2 a new curvature estimator based on Maximal Digital Circular Arcs detection (MDCA). It is thus a natural extension of uniformly convergent tangent estimators based on maximal DSS [11]. It is a parameter-free method, with linear computation time in practice. Section 3 discuss the multigrid convergence of this estimator and establishes the importance of the asymptotic length evolution of MDCAs as the resolution gets finer. Section 4 verifies experimentally the asymptotic behavior of MDCAs and of the curvature field estimation. These results backs up our claim that this estimator is multigrid-convergent. Section 5 compares numerically this estimator with the latest curvature estimators of the literature: the binomial convolution (BC) estimator of [13,3], and the global min-curvature (GMC) estimator of [9]. They show that this new estimator outperforms the previous ones on tested shapes.

2 Curvature Estimation Based on the Set of Maximal Digital Circular Arcs

We propose in this section a curvature estimator based on a curvature map computed from the set of maximal digital circular arcs.

Let $\mathbb{X}$ be a family of compact simply connected subsets of $\mathbb{R}^2$ with continuous curvature fields. The reason that explains why we need continuous curvature fields is postponed to section 3.1. We denote by $D_h(X)$ the Gauss digitization of $X \in \mathbb{X}$ with grid step h, seen as a union of pixels of side h in $\mathbb{R}^2$. For sake of clarity, we shorten in the sequel $D_h(X)$ into D and denote its complementary by $\bar{D}$. Moreover, let us assume that D contains at least one pixel, i.e. $|D| \geq 1$.

Let the *digital contour* C of D be the topological border ∂D of D. Any side of any pixel is a *grid edge*. The contour C is a circular list of grid edges in the clockwise orientation. Any part C' of C is a sequence of consecutive grid edges. The *discrete length* of C' is defined as its number of grid edges. The distance between two grid edges is defined as the discrete length of the shortest part joining these two grid edges. Each grid edge lies between two pixels, one belonging to D, the other belonging to $\bar{D}$. The centers of the pixels incident to C' and belonging to D are the *interior points* of C', whereas those of the pixels incident to C' and belonging to $\bar{D}$ are the *exterior points* of C'.

Any part C' of C is a *digital circular arc* (DCA for short) if and only if the interior and exterior points of C' are circularly separable, i.e. there exists a (Euclidean) circle that either encloses the interior points without enclosing any exterior points or that encloses the exterior points without enclosing any interior points. Given a grid step h, the map associating to any DCA A the value 0 if the interior and exterior points of A are linearly separable and the curvature of an arbitrary separating circle otherwise is denoted by k^h, such that $k^h(A)$ is the curvature of the part A (and h is the unit).

Any DCA A is maximal if and only if all the parts C' containing A, i.e. such that $A \subset C'$, are not a DCA. The set of all maximal DCAs (MDCAs for short) that lie on a given contour is unique. The first grid edge of any two distinct MDCAs cannot be identical because if it is, the shortest MDCA is necessarily contained in the longest one and is thus not maximal. Consequently, the MDCAs can be ordered according to the position of their first grid edge in the contour. Let us then denote by $(A_i)_{i\in 1,\dots,n}$ the sequence of the n MDCAs lying on C.

Given any DCA A of discrete length L, the map associating A to its middle grid edge is denoted by m such that $m(A)$ is the $\lceil \frac{L}{2} \rceil$-th grid edge of A. Note that the middle grid edges of any two consecutive MDCA are never the same grid edge.

As a result, a contour C can be partitioned without ambiguity into a sequence $(V_i)_{i\in 1,\dots,n}$ such that V_i is the set of grid edges closer to $m(A_i)$ than to any other grid edge $m(A_j)$, $j \in 1,\dots,n$ and $j \neq i$ (the first one with respect to the clockwise orientation of the contour is assumed to be closer in case of tie). For all $i \in 1,\dots,n$, we associate to any grid edge of V_i, the curvature value of the separating circle associated to the MDCA A_i.

Definition 1. *Let $(A_i)_{i\in 1,n}$ be the sequence of MDCAs lying on C. Let $(V_i)_{i\in 1,n}$ be a partition of C such that V_i is the set of grid edges closer to $m(A_i)$ than to any other grid edge $m(A_j)$, $j \in 1,\dots,n$ and $j \neq i$ Given a grid step h, the* curvature estimator $\hat{\kappa}^h_{MDCA}$ *is the piecewise constant function that associates to any digital contour C and to any point p of C a curvature value in $\mathbb{R}$ such that:*

$$\forall i \in 1,\dots,n, \forall e \in V_i, \forall p \in e, \hat{\kappa}^h_{MDCA}(C,p) = k^h(A_i).$$

A minimal example is provided in Fig. 1.

3 On the Multigrid Convergence of the MDCA Estimator

In this section, we first propose a discrete curvature estimator definition and next discuss of the multigrid convergence properties of $\hat{\kappa}_{MDCA}$.

3.1 Multigrid Convergence Definition for a Curvature Estimator

The curvature is some function of the shape boundary. However, the contour of the shape digitization does not define the same domain. Therefore we cannot directly compare the true curvature function with the estimated curvature

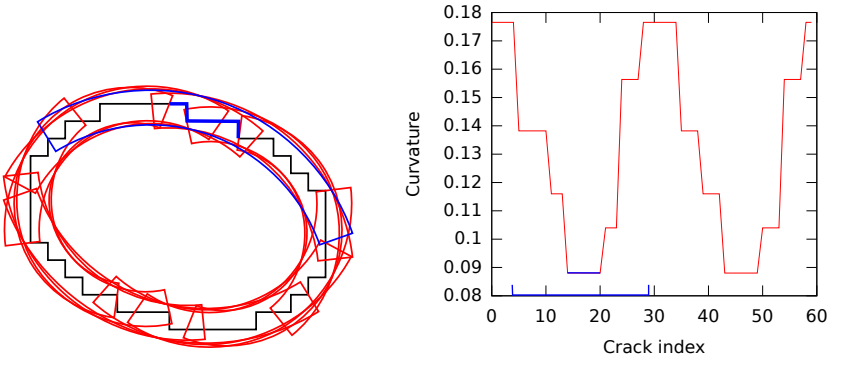

(a) (b)

Fig. 1. The set of MDCAs (12 arcs) is depicted in a) with pieces of rings along the contour of the digitization of an ellipse having a great axis of 9 pixels long and a small axis of 6 pixels long. The angle between the main orientation and the x-axis is equal to 1.9 radians. The curvature plot defined from the set of MDCAs is shown in b). The blue grid edges are those whose curvature depends on the radius of the blue MDCA.

function. We provide below a definition of multigrid convergence for discrete curvature estimators. It is neither a parametric definition as in [3] nor a pointwise definition as the standard multigrid convergence reported in [10]. It is a geometric definition, stating that any digital point sufficiently close to the point of interest has its estimated curvature which tends toward the expected curvature. This definition of multigrid convergence imposes shapes with continuous curvature fields.

Let us recall that $\mathbb{X}$ is a family of compact simply connected subsets of $\mathbb{R}^2$ with continuous curvature field. We denote by $D_h(X)$ the Gauss digitization of $X \in \mathbb{X}$ with grid step h. For any x in the topological boundary ∂X of X, let $\kappa(X, x)$ be the curvature of ∂X at x. A *discrete curvature estimator* $\hat{\kappa} = (\hat{\kappa}^h)_{h>0}$ is a family of mappings which associates to any digital contour C and a point $p \in C$ some value of $\mathbb{R}$. Note that the estimator proposed in Definition 1, is a discrete curvature estimator as defined above. The following section aims at studying the multigrid-convergence of this estimator:

Definition 2. *The estimator $\hat{\kappa}$ is* multigrid-convergent *for the family $\mathbb{X}$ if and only if, for any $X \in \mathbb{X}$, $h > 0$, for any $x \in \partial X$,*

$$\forall y \in \partial D_h(X) \text{ with } \|y - x\|_1 \leq h, |\hat{\kappa}^h(D_h(X), y) - \kappa(X, x)| \leq \tau_x(h),$$

where $\tau_{X,x} : \mathbb{R}^{+*} \to \mathbb{R}^+$ has null limit at 0. This function defines the speed of convergence of $\hat{\kappa}$ toward κ at point x of X. The convergence is uniform *for X*

when every $\tau_{X,x}$ is bounded from above by a function τ_X independent of $x \in X$ with null limit at 0.

3.2 Relation with Growth of MDCAs

In this section, we establish a link between the multigrid convergence of our estimator and the asymptotic length of the MDCAs along the digital shape. We restrict our study to convex shapes having strictly positive and finite curvature.

We recall first that any convex shape X is uniquely determined by its *support function* f of center B, with $f : [0, 2\pi[\to \mathbb{R}$. In our case, $f(\phi)$ is the algebraic distance between B and the point of ∂X with normal $\boldsymbol{n}(\phi) = (\cos\phi, \sin\phi)$. A (θ_1, θ_2)-*piece of* (B, R, e)-*ring* is the subset of $\mathbb{R}^2$ defined in polar coordinates as $\{(r, \theta) : R - e \leq r \leq R + e, \theta_1 \leq \theta \leq \theta_2\}$. It is said to be *simply covering* ∂X if its intersection with ∂X is a simple curve whose extremities have a polar angle of respectively θ_1 and θ_2.

Lemma 1. *Let $\mathcal{R}$ be a (θ_1, θ_2)-piece of (B, R, h)-ring that simply covers ∂X, whose Euclidean length $R(\theta_2 - \theta_1)$ is lower bounded by $\Omega(h^a)$ and upper bounded by $O(h^b)$, $0 < b \leq a < 1/2$. Then, the radius R tends towards the inverse of the curvature of ∂X at any points of $\mathcal{R} \cap \partial X$ as $h \to 0$.*

Proof. Let $\mathcal{R}$ be such a ring. Its length is $L = R(\theta_2 - \theta_1)$. The points of ∂X at θ_1 and θ_2 are respectively denoted by M_1 and M_2. The points M_i, $i = 1, 2$, have normals $\boldsymbol{n}(\phi_i)$. We represent X with its support function f centered on B. We proceed in four steps.

1. We relate $\theta_2 - \theta_1$ and $\phi_2 - \phi_1$.
   Let L_{12} be the length ∂X between M_1 and M_2. By convexity of X, L_{12} is longer than the shortest arc of $\mathcal{R}$ and shorter than the longest arc of $\mathcal{R}$ plus twice its thickness. We get:

   $$(R - h)(\theta_2 - \theta_1) \leq L_{12} \leq (R + h)(\theta_2 - \theta_1) + 4h$$

   But $L_{12} = \int_{\phi_1}^{\phi_2} \frac{1}{\kappa} d\phi$. Introducing $\kappa_{\min}$ and $\kappa_{\max}$ as a lower and upper bound on the curvature in $\partial X \cap \mathcal{R}$, we easily get by integration:

   $$\kappa_{\min}(R - h)(\theta_2 - \theta_1) \leq \phi_2 - \phi_1 \leq \kappa_{\max}((R + h)(\theta_2 - \theta_1) + 4h),$$

   and since $L/R = \theta_2 - \theta_1$:

   $$\kappa_{\min}(1 - h/R)L \leq \phi_2 - \phi_1 \leq \kappa_{\max}((1 + h/R)L + 4h), \tag{1}$$

2. We major f'' at point $\overline{M} \in \partial X$ whose normal has angle $\overline{\phi} = (\phi_1 + \phi_2)/2$. Finite differences applied on $f''(\overline{\phi})$ gives:

   $$f''(\overline{\phi}) = \frac{f(\phi_1) - 2f(\overline{\phi}) + f(\phi_2)}{((\phi_2 - \phi_1)/2)^2} + O(\phi_2 - \phi_1). \tag{2}$$

Since $M_1, \overline{M}, M_2$ are all in $\mathcal{R}$ and since the support function f has center B, the values $f(\phi_1), f(\overline{\phi}), f(\phi_2)$ are bounded by $R-h$ and $R+h$. We also insert (1) in (2) to get:

$$|f''(\overline{\phi})| \leq \frac{16h}{\kappa_{\min}^2 L^2} \left(\frac{1}{1+O(h/R)} \right) + O(L(1+h/R)) + O(h). \tag{3}$$

3. The quantity $f''(\overline{\phi})$ tends toward 0 as $h \to 0$.
The radius R of the ring is lower bounded by some constant for sufficiently small h since ∂X has finite curvature everywhere. As a result $h/R \to 0$ as $h \to 0$. We insert the hypothesis $\Omega(h^a) \leq L \leq O(h^b)$ into (3):

$$|f''(\overline{\phi})| \leq O(h^{1-2a}) + O(h^b) + O(h). \tag{4}$$

From $1/2 > a$ and $0 < b$, it is clear that $|f''(\overline{\phi})|$ tends toward 0 as $h \to 0$.
4. We relate the behavior of f'' to the curvature.
It is well known that the curvature has a close relation with the support function: $\forall \phi, 1/\kappa(\phi) = f(\phi) + f''(\phi)$. Now $\forall \phi, \phi_1 \leq \phi \leq \phi_2$, we have $R-h \leq f(\phi) \leq R+h$. This holds also for $\overline{\phi}$ which lies between ϕ_1 and ϕ_2. We immediately obtain

$$1/\kappa(\overline{\phi}) = R + O(h) + O(f''(\overline{\phi})). \tag{5}$$

From (4) and (5), it is now obvious that the radius of the covering ring tends toward the inverse of the curvature of some point in $\mathcal{R} \cap \partial X$. The curvature of ∂X being continuous and $\mathcal{R}$ being included in some ball of radius $O(h^b)$, $b > 0$, the same holds for all points of $\mathcal{R} \cap \partial X$. □

It remains to show that there always exists a piece of ring simply covering ∂X for any MDCA.

Theorem 1. *Let $\mathbb{X}$ be the family of compact convex subsets of $\mathbb{R}^2$, whose curvature field is continuous, strictly positive and upper bounded. If the length of MDCAs along any $D_h(X)$, $X \in \mathbb{X}$, is lower bounded by $\Omega(h^a)$ and upper bounded by $O(h^b)$, $0 < b \leq a < 1/2$, then the curvature estimator $\hat{\kappa}_{MDCA}$ is uniformly multigrid convergent for X, with $\tau = O(h^{\min(1-2a,b)})$.*

Proof. Let $h > 0$, $x \in \partial X$, and $y \in \partial D_h(X), \|y - x\|_1 \leq h$. The point y is closer to some MDCA A_i than to any other one. Let $\mathcal{C}$ be any circle separating the interior and exterior points of A_i. Let us denote by B its center and R its radius. Let θ_1 and θ_2 be the polar angle (with respect to B) of the extremities of A_i. Let $\mathcal{R}$ be the (θ_1, θ_2)-piece of $(B, R, \sqrt{2}h)$-ring. See Fig. 2 for an illustration. The circle $\mathcal{C}$ separates all the interior points from the exterior points of A_i. Since we have chosen the width $\sqrt{2}h$, we also know that all these points are included in $\mathcal{R}$. Since ∂X is contained in the one-pixel wide strip between interior and exterior points of the grid edges, ∂X can only exit $\mathcal{R}$ on its sides. It is well known that for a sufficiently small h, the digital contour $\partial D_h(X)$ has the same topology as ∂X (e.g. par-regularity [7]). Therefore $\partial X \cap \mathcal{R}$ has the same topology as $\partial D_h(X) \cap \mathcal{R}$,

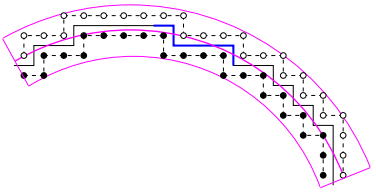

Fig. 2. Illustration of the proof of Theorem 1: piece of ring defined from the separating circle of a given MDCA

i.e. it is curve without intersection. We conclude that $\mathcal{R}$ is simply covering ∂X. By definition $\mathcal{R}$ covers y, but also x: indeed, it is the most centered MDCA, and an MDCA is at least longer than three pixels. Applying Lemma 1, gives that the inverse of R tends toward the curvature at x, and more precisely in $O(h^{\min(1-2a,b)})$ according to (4). We conclude since $\hat{\kappa}_{MDCA}$ gives by definition $1/R$ at y. □

If $N = 1/h$ is the resolution, The discrete length of MDCAs (length divided by h) must thus grow at speed faster than $\Omega(h^{-\frac{1}{2}})$, i.e. $\Omega(\sqrt{N})$, and smaller than $O(h^{-1})$, i.e. $O(N)$, so that the curvature estimator $\hat{\kappa}_{MDCA}$ is multigrid convergent.

4 Experimental Evaluation

We experimentally observed on digitizations of ellipses that the average discrete length of the MDCAs grows in $\Theta(h^{-\frac{1}{2}})$ as h tends towards 0 (Fig. 3.a). According to the results of the previous section, this suggests that the proposed estimator is multigrid convergent for strictly convex shapes having continuous curvature fields such as ellipses.

In order to observe the multigrid convergence of our estimator for an ellipse E of center c, we compared the value of $\hat{\kappa}^h_{MDCA}$ to the ground-truth $\hat{\kappa}$. For each grid edge, we associated to the midpoint p, its projection p' on ∂E along the ray coming from c so that the absolute error at p is defined as:

$$\epsilon_{abs}(p) = |\hat{\kappa}(\partial E, p') - \hat{\kappa}^h_{MDCA}(\partial D_h(E), p)| \tag{6}$$

The relative error at p is consequently defined as:

$$\epsilon_{rel}(p) = \frac{\epsilon_{abs}(p)}{\hat{\kappa}(\partial E, p')} \tag{7}$$

The average absolute and relative error have been plotted against the grid step h in Fig. 3.b. We experimentally observed that the convergence speed is $\Theta(h^{\frac{1}{2}})$.

Note however that the discrete length of the smallest MDCA grows more likely in $\Theta(h^{-0.43})$ (Fig. 3.a), which means that the proposed estimator may not be *uniformly* convergent.

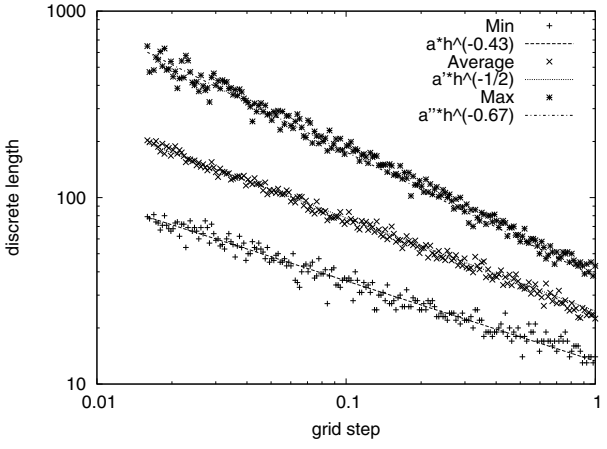

(a)

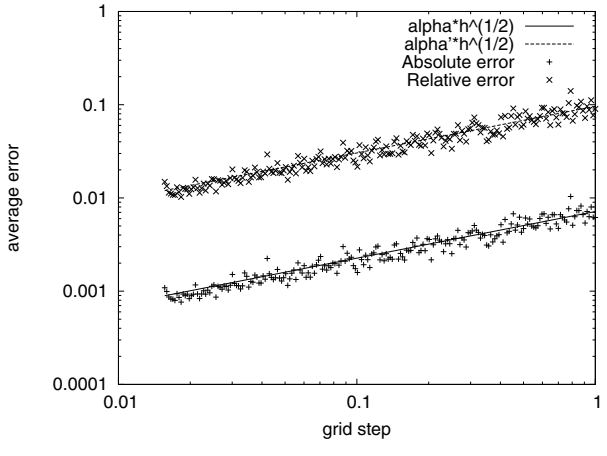

(b)

Fig. 3. The set of MDCAs has been computed from the contour of the digitization of an ellipse of elongation $\frac{1}{3}$. The minimal, average and maximal discrete length of the MDCAs have been plotted against the grid step h in (a). The average absolute and relative error have been plotted against the grid step h in (b).

The position and the orientation of the ellipses have no significant impact on the discrete length of the MDCAs (and as expected, the finer the resolution is, the smaller the variation is). The elongation of the ellipses has however an impact on the magnitude of the discrete length of the MDCAs. We set the great

axis of an ellipse to 24 pixels and set the small one to 6, 8, 12, 16 and 18 pixels, in order to test ellipses of elongation $\frac{1}{4}$, $\frac{1}{3}$, $\frac{1}{2}$, $\frac{2}{3}$ and $\frac{3}{4}$ respectively. In either case, the average discrete length of the MDCAs grows in $\Theta(h^{-\frac{1}{2}})$ as h tends towards 0. Though, for a given great axis, the larger the small axis is, the higher the average discrete length of the MDCAs is.

5 Comparisons

We report below the comparison of our estimator to the latest curvature estimators of the literature for three shapes: a disk of radius 15, an ellipse of great (resp. small) axis 30 (resp. 20) and a flower of five petals, of great (resp. small) radius 15 (resp. 10).

These shapes have been digitized (according to Gauss scheme) at three different grid steps: $h = 1$, $h = 0.1$ and $h = 0.01$. The digital objects obtained for $h = 1$ and $h = 0.1$ are depicted Fig. 4. Their digital contour is the input of the curvature estimation methods.

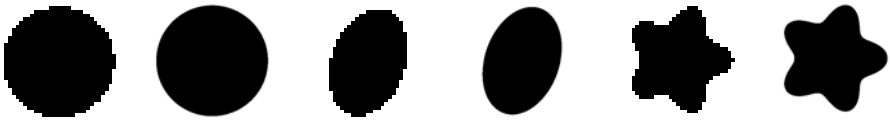

(a) 1 (b) 0.1 (c) 1 (d) 0.1 (e) 1 (f) 0.1

Fig. 4. Digitization at two different grid steps of the circle (a-b), the ellipse (c-d) and the flower (e-f) for which the curvature has been estimated

5.1 Implementation Issues

The GMC estimator [9] computes the shape whose digitization coincides with the input digital object and that minimizes its squared curvature. The minimization is performed by an iterative numerical technique that stops when the difference between the squared curvature of the last two solution shapes is less than a small quantity set to 1.10^{-8} in what follows.

The BC estimator [13,3] is computed from derivative estimations, get by finite differences after the convolution of the contour points by a binomial kernel of a given size. The mask size is an input parameter that is not easy to determine, but following [13], it has been set to $d.h^{\frac{4}{3}}$ where d is the diameter of the shape, equal here to 30 for the circle, the ellipse and the flower.

As explained in Section 2, the proposed estimator is computed from the set of MDCAs.

For the recognition of the DCAs, we use the on-line algorithm proposed in [15]. The algorithm incrementally computes one (Euclidean) circle that separates the

interior and exterior points of a DCA and that is called below *current circle*. Deciding whether a DCA can be extended to a new grid edge requires to check the location of the interior and exterior points of the grid edge with respect to the current circle. If the interior (resp. exterior) point is located inside (resp. outside) the current circle, nothing has to be done because the current circle is still separating. However, if the interior (resp. exterior) point is located outside (resp. inside) the current circle, then either the point is located on another separating circle, or the sets of interior and exterior points are not circularly separable at all. A linear-time procedure, which computes the set of separating circles passing through a given point, is used in the aim of deciding between these two alternatives. A naive upper bound for the extension of a DCA to a new grid edge is thus $O(n)$, but we experimentally observe a constant time in average because the linear-time procedure is called only a few times.

The set of MDCAs is then computed DCA by DCA using the above recognition algorithm and following the scheme given in [4] for the maximal digital straight segments. The mechanism can be coarsely described as follows: given a MDCA A_i and the first grid edge e following A_i, the next MDCA A_j is computed in two steps. First, we compute the longest DCA starting from e and scanning the contour backward. Then, we extend this DCA forward as far as possible until it is maximal. The number of times we try to extend a DCA is bounded by the sum of the discrete length of the MDCAs. We experimentally observe that this sum is proportional to the length of the contour and that the global complexity the MDCAs computation is linear in practice.

5.2 Accuracy and Running Time

In Fig. 5, we compare the curvature plots derived from the MDCA, GMC and BC estimators to the ground-truth. The visual deviation between the estimated graphs and the ground-truth graph reflects the average absolute error available in Tab. 1. For either estimator, the curvature estimations are more accurate for the circle than for the ellipse and more accurate for the ellipse than for the flower. For either shape, the GMC and MDCA estimations gets closer to the ground-truth (Fig. 5) and their absolute error decreases (Tab. 1) as h decreases. However, the BC estimations are not improved by increasing the resolution, except for the flower. Lastly, MDCA estimations are always better than GMC and BC estimations except in one case (maximal error for the flower at grid step 0.01), even by several orders of magnitude for the circle. For the ellipse and the flower, at grid step 0.01, MDCA estimations are 4 times better than GMC estimations in average and much more better than BC estimations (Tab. 1). In Fig. 5, the MDCA graph is hardly confounded with the ground-truth graph.

Tab. 2 reports the running times. The algorithms have been implemented in C++ and have been run on an Intel Core Duo processor work-station with a 2.4 GHz Clock and 2GB of main memory.

The running times of the BC estimator grow quickly as h decreases and is high at grid step 0.01 (18s) because the mask size must be set to $d.h^{4/3}$. The GMC estimator and leads to rather low running times, minimal for the flower (823ms

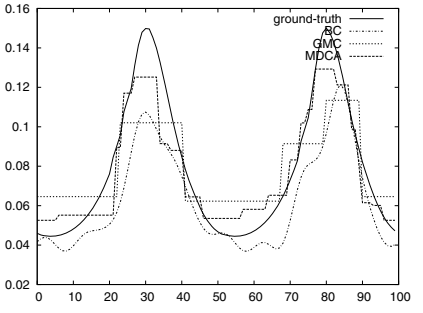

(a) ellipse, $h = 1$

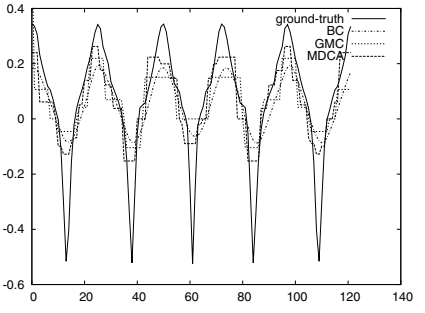

(b) flower, $h = 1$

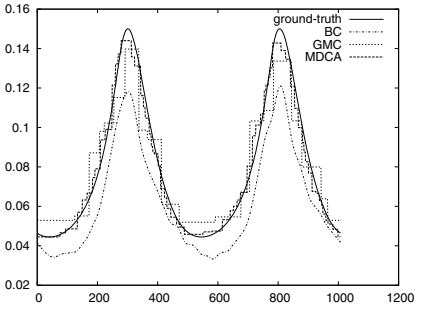

(c) ellipse, $h = 0.1$

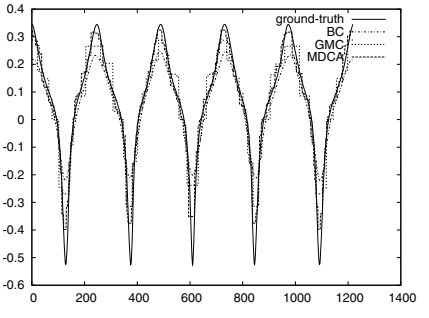

(d) flower, $h = 0.1$

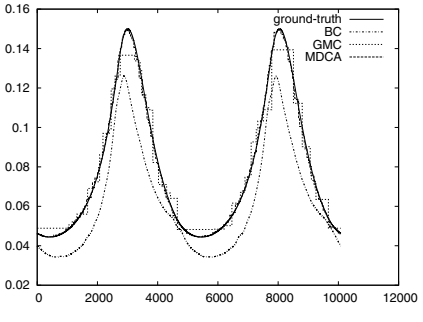

(e) ellipse, $h = 0.01$

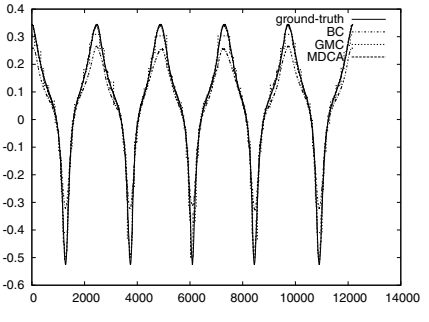

(f) flower, $h = 0.01$

Fig. 5. Curvature plots for two shapes digitized at three different resolutions, computed from the proposed estimator (MDCA) and the latest curvature estimators of the literature (BC [13,3] and GMC [9])

Table 1. Average and maximal absolute error of the curvature estimation for three shapes digitized at three different grid steps and comparisons with the BC and GMC estimators

		circle			ellipse			flower		
h		1	0.1	0.01	1	0.1	0.01	1	0.1	0.01
♯ grid edges		120	1200	12000	100	1008	10078	122	1220	12184
BC	avg	0.0143	0.0143	0.0143	0.0168	0.0170	0.0170	0.1044	0.0623	0.0440
	max	0.0262	0.0205	0.0203	0.0577	0.3634	0.0389	0.4648	0.3236	0.2143
GMC	avg	8.10^{-4}	3.10^{-5}	3.10^{-5}	0.0168	0.0086	0.0044	0.1103	0.0519	0.0222
	max	5.10^{-3}	4.10^{-5}	9.10^{-5}	0.0562	0.0336	0.0281	0.5250	0.2869	0.1529
MDCA	avg	4.10^{-5}	5.10^{-7}	8.10^{-8}	0.0094	0.0034	0.0009	0.0845	0.0281	0.0084
	max	4.10^{-5}	5.10^{-7}	8.10^{-8}	0.0413	0.0149	0.0068	0.4356	0.1918	0.1552

Table 2. Running time of the curvature estimation for three shapes digitized at three different grid steps and comparisons with the BC and GMC estimators

		circle			ellipse			flower		
h		1	0.1	0.01	1	0.1	0.01	1	0.1	0.01
♯ grid edges		120	1200	12000	100	1008	10078	122	1220	12184
timing (ms)	BC	< 1	63	18596	< 1	55	30197	< 1	83	18704
	GMC	< 1	820	2360	< 1	27	1843	< 1	15	843
	MDCA	< 1	23	455	7	139	1783	3	127	2195

at 0.01) and maximal for the circle (2360ms at 0.01). The MDCA estimator is linear-time in practice and also leads to low running times, minimal for the circle (455ms at 0.01) and maximal for the flower (2195ms at 0.01). It is the best method when averaging over the three shapes.

6 Conclusion and Perspectives

The proposed estimator does not require any parameter, is fast to compute (linear-time in practice) and more accurate than the latest estimators of the literature at low as well as high resolution. We provide a necessary condition about the length of the maximal digital circular arcs under which the proposed estimator is multigrid convergent. We experimentally observed that this condition is fulfilled and proving this fact is our main perspective. We are also interested in dealing with shapes corrupted by noise in a multi-resolution framework.

References

1. Coeurjolly, D., Miguet, S., Tougne, L.: Discrete curvature based on osculating circle estimation. In: Arcelli, C., Cordella, L.P., Sanniti di Baja, G. (eds.) IWVF 2001. LNCS, vol. 2059, pp. 303–312. Springer, Heidelberg (2001)

2. Coeurjolly, D., Svensson, S.: Estimation of curvature along curves with application to fibres in 3D images of paper. In: Bigun, J., Gustavsson, T. (eds.) SCIA 2003. LNCS, vol. 2749, pp. 247–254. Springer, Heidelberg (2003)
3. Esbelin, H.-A., Malgouyres, R.: Convergence of binomial-based derivative estimation for c2- noisy discretized curves. In: Brlek, S., Reutenauer, C., Provençal, X. (eds.) DGCI 2009. LNCS, vol. 5810, pp. 57–66. Springer, Heidelberg (2009)
4. Feschet, F., Tougne, L.: Optimal time computation of the tangent of a discrete curve: Application to the curvature. In: Bertrand, G., Couprie, M., Perroton, L. (eds.) DGCI 1999. LNCS, vol. 1568, pp. 31–40. Springer, Heidelberg (1999)
5. Fiorio, C., Mercat, C., Rieux, F.: Curvature estimation for discrete curves based on auto-adaptive masks of convolution. In: Barneva, R.P., Brimkov, V.E., Hauptman, H.A., Natal Jorge, R.M., Tavares, J.M.R.S. (eds.) CompIMAGE 2010. LNCS, vol. 6026, pp. 47–59. Springer, Heidelberg (2010)
6. Fleischmann, O., Wietzke, L., Sommer, G.: A Novel Curvature Estimator for Digital Curves and Images. In: Goesele, M., Roth, S., Kuijper, A., Schiele, B., Schindler, K. (eds.) DAGM 2010. LNCS, vol. 6376, pp. 442–451. Springer, Heidelberg (2010)
7. Gross, A., Latecki, L.: Digitizations preserving topological and differential geometric properties. Comput. Vis. Image Underst. 62(3), 370–381 (1995)
8. Hermann, S., Klette, R.: A comparative study on 2d curvature estimators. In: Proc. ICCTA, pp. 584–589 (2007)
9. Kerautret, B., Lachaud, J.-O.: Curvature estimation along noisy digital contours by approximate global optimization. Pattern Recognition 42(10), 2265–2278 (2009)
10. Klette, R., Rosenfeld, A.: Digital Geometry - Geometric Methods for Digital Picture. Morgan Kaufmann, San Francisco (2004)
11. Lachaud, J.-O., Vialard, A., de Vieilleville, F.: Fast, accurate and convergent tangent estimation on digital contours. Image and Vis. Comput. 25(10), 1572–1587 (2007)
12. Liu, H., Latecki, L., Liu, W.: A unified curvature definition for regular, polygonal, and digital planar curves. Int. Jour. of Comput. Vis. 80, 104–124 (2008)
13. Malgouyres, R., Brunet, F., Fourey, S.: Binomial convolutions and derivatives estimation from noisy discretizations. In: Coeurjolly, D., Sivignon, I., Tougne, L., Dupont, F. (eds.) DGCI 2008. LNCS, vol. 4992, pp. 370–379. Springer, Heidelberg (2008)
14. Marji, M.: On the detection of dominant points on digital planar curves. PhD thesis, Wayne State University, Detroit, Michigan (2003)
15. Roussillon, T., Sivignon, I., Tougne, L.: On three constrained versions of the digital circular arc recognition problem. In: Brlek, S., Reutenauer, C., Provençal, X. (eds.) DGCI 2009. LNCS, vol. 5810, pp. 34–45. Springer, Heidelberg (2009)
16. Vialard, A.: Geometrical parameters extraction from discrete paths. In: Miguet, S., Ubéda, S., Montanvert, A. (eds.) DGCI 1996. LNCS, vol. 1176, pp. 24–35. Springer, Heidelberg (1996)
17. Worring, M., Smeulders, A.W.M.: Digital curvature estimation. CVGIP: Image Understanding 58(3), 366–382 (1993)